

# Threshold-activated transport stabilizes chaotic populations to steady states

Chandrakala Meena, Pranay Deep Rungta, Sudeshna Sinha\*

Department of Physical Sciences, Indian Institute of Science Education and Research (IISER) Mohali, Knowledge City, SAS Nagar, Sector 81, Manauli PO 140306, Punjab, India.

\*sudeshna@iisermohali.ac.in

## Abstract

We explore Random Scale-Free networks of populations, modelled by chaotic Ricker maps, connected by transport that is triggered when population density in a patch is in excess of a critical threshold level. Our central result is that threshold-activated dispersal leads to stable fixed populations, for a wide range of threshold levels. Further, suppression of chaos is facilitated when the threshold-activated migration is more rapid than the intrinsic population dynamics of a patch. Additionally, networks with large number of nodes open to the environment, readily yield stable steady states. Lastly we demonstrate that in networks with very few open nodes, the degree and betweenness centrality of the node open to the environment has a pronounced influence on control. All qualitative trends are corroborated by quantitative measures, reflecting the efficiency of control, and the width of the steady state window.

## Introduction

Nonlinear systems, describing both natural phenomena as well as human-engineered devices, can give rise to a rich gamut of patterns ranging from fixed points to cycles and chaos. So mechanisms that enable a chaotic system to maintain a fixed desired activity (the “goal”) has witnessed enormous research attention [1]. In early years the focus was on controlling low-dimensional chaotic systems, and guiding chaotic states to desired target states [2–4]. Efforts then moved on to the arena of lattices modelling extended systems, and the control of spatiotemporal patterns in such systems [5]. With the advent of network science to describe connections between complex sub-systems, the new challenge is to find mechanisms or strategies that are capable of stabilizing these large interactive systems [6].

In this work we consider a network of population patches [7,8], or “a population of populations” [9]. Now, most models of metapopulation dynamics consider density dependent dispersal, analogous to reaction-diffusion processes [10–14]. Here we consider a different scenario, namely one where the inter-patch connection is triggered by the excess of population density in a patch [4,15]. This describes a system comprising of many spatially discrete sub-populations connected by threshold-activated dispersal. Our principal question will be the following: *can threshold-activated coupling serve to control networks of intrinsically chaotic populations on to regular behaviour?*

In the sections below, we will first discuss details of the nodal dynamics, as well as the salient features of pulsatile transport triggered by threshold mechanisms. We will

then go on to demonstrate, through qualitative and quantitative measures, that such threshold-activated connections manage to stabilize chaotic populations to steady states. Further we will explore how the critical threshold that triggers the migration, and the timescales of the nodal dynamics vis-a-vis transport, influences the emergent dynamics.

## Model

Consider a network of  $N$  sub-systems, characterized by variable  $x_n(i)$  at each node/site  $i$  ( $i = 1, \dots, N$ ) at time instant  $n$ . Specifically, we study a prototypical map, the Ricker (Exponential) Map, at the local nodes. Such a map models population growth of species with non-overlapping generations, and is given by the functional form:

$$x_{n+1}(i) = f(x_n(i)) = x_n(i) \exp(r(1 - x_n(i))) \quad (1)$$

where  $r$  is interpreted as an intrinsic growth rate and (dimensionless)  $x_n(i)$  is the population scaled by the carrying capacity at generation  $n$  at node/site  $i$ . We consider  $r = 4$  in this work, namely, an isolated uncoupled population patch displays *chaotic* behaviour.

The coupling in the system is triggered by a threshold mechanisms [4, 16, 17]. Namely, the dynamics of node  $i$  is such that if  $x_{n+1}(i) > x_c$ , the variable is adjusted back to  $x_c$  and the “excess”  $x_{n+1} - x_c$  is distributed to the neighbouring patches. The threshold parameter  $x_c$  is the critical value the state variable has to exceed in order to initiate threshold-activated coupling. So this class of coupling is *pulsatile*, rather than the more usual continuous coupling forms, as it is triggered *only* when a node exceeds threshold.

Specifically, we study such population patches coupled in a Random Scale-Free network, where the network of underlying connections is constructed via the Barabasi-Albert preferential attachment algorithm, with the number of links of each new node denoted by parameter  $m$  [18]. The resultant network is characterized by a fat-tailed degree distribution, found widely in nature. The underlying web of connections determines the “neighbours” to which the excess is equi-distributed. Further, certain nodes in the network may be open to the environment, and the excess from such nodes is transported out of the system. Such a scenario will model an open system, and such nodes are analogous to the “open edge of the system”. We denote the fraction of open nodes in the network, that is the number of open nodes scaled by system size  $N$ , by  $f^{open}$ . In this work we also consider closed systems with no nodes open to the environment, where nothing is transported out of the system, i.e.  $f^{open} = 0$ .

The threshold-activated migration from an over-critical patch can trigger subsequent transport, as the redistribution of excess can cause neighbouring sites to become over-critical, thus initiating a domino effect, much like an “avalanche” in models of self-organized criticality [19]. All transport within patches stop when all patches are under the critical value, i.e. all  $x(i) < x_c$ . So there are two natural time-scales here. One time-scale characterizes the chaotic update of the populations at node  $i$ . The other time scale involves the redistribution of population densities arising from threshold-activated transport. We denote the time interval between chaotic updates, namely the time available for redistribution of excess resulting from threshold-activated transport processes, by  $T_R$ . This is analogous to the *relaxation time* in models of self-organized criticality, such as the influential sandpile model [19].  $T_R$  then indicates the comparative time-scales of the threshold-activated migration and the intrinsic population dynamics of a patch.

## Results

We have simulated this threshold-coupled scale-free network of populations, under varying threshold levels  $x_c$  ( $0 \leq x_c \leq 2$ ). We considered networks with varying number of open nodes, namely systems that have different nodes/sites open to the environment from where the excess population can migrate out of the system. Further, we have studied a range of redistribution times  $T_R$ , capturing different timescales of migration vis-a-vis population change [20]. With no loss of generality, in the sections below, we will present salient results for Random Scale-Free networks with  $m = 1$ , and specifically demonstrate, both qualitatively and quantitatively, the stabilization of networks of chaotic populations to steady-states under threshold-activated coupling.

### Emergence of Steady States

First, we consider the case of large  $T_R$ , where the transport processes are fast compared to the population dynamics, or equivalently, the population dynamics of the patch is slow compared to inter-patch migrations. Namely, since the chaotic update is much slower than the transport between nodes, the situation is analogous to the slow driving limit [19]. In such a case, the system has time for many transport events to occur between chaotic updates, and avalanches can die down, i.e. the system is “relaxed” or “under-critical” between the chaotic updates. So when the transport/migration is significantly faster than the population update (namely the time between generations), the system tends to reach a stationary state where all nodal populations are less than critical.

An illustrative case of the state of the nodes in the network is shown in Fig. 1. Without much loss of generality, we display results for a network of size  $N = 100$ , for a representative large value of redistribution time  $T_R = 5000$ . It is clear that *all the nodes in the network gets stabilized to a fixed point*, namely all population patches evolve to a stable steady state.

The next natural question is the influence of the critical threshold  $x_c$  on the emergent dynamics. This dependence is demonstrated in bifurcation diagrams displayed in Fig. 2. It is clearly evident from these that a *large window of threshold values* ( $0 \leq x_c < 1$ ) yield spatiotemporal steady states in the network [21]. It is also apparent that the degree of the open node does not affect the emergence of steady states here. Further, for threshold values beyond the window of control to fixed states, one obtains cycles of period 2. Namely for threshold levels  $1 < x_c < 2$  the populations evolve in regular cycles, where low population densities alternate with a high population densities. This behaviour is reminiscent of the field experiment conducted by Scheffer et al [22] which showed the existence of self-perpetuating stable states alternating between blue-green algae and green algae. We discuss the underlying reason for this behaviour in the Appendix, and offer analytical reasons for the range of period-1 and 2 behaviour considering a single threshold-limited map.

So our first result can be summarized as follows: when redistribution time  $T_R$  is large and the critical threshold  $x_c$  is small, we have very efficient control of networks of chaotic populations to steady states. This suppression of chaos and quick evolution to a stable steady states occurs irrespective of the number of open nodes.

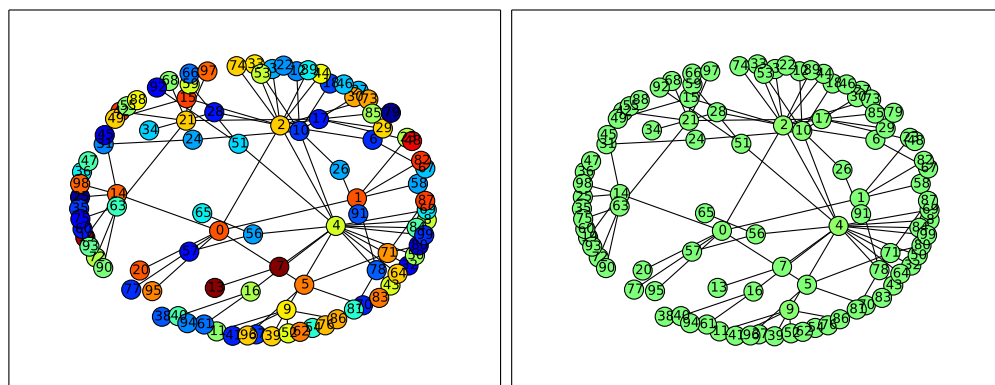


**Fig 1. State of the nodes (coded in color) in a Random Scale-Free Network of intrinsically chaotic populations under threshold-activated coupling, at different instants of time.** Here the steady state value represented by the light green color. The left panel displays the network at initial time, showing the random initial state of the network. The right panel shows the network after 50 time steps, clearly showing that all nodes have evolved to a steady state (as evident from the uniform light green color). Here redistribution time  $T_R = 5000$  and the critical threshold  $x_c = 0.5$ , and there is a single node open to the environment.

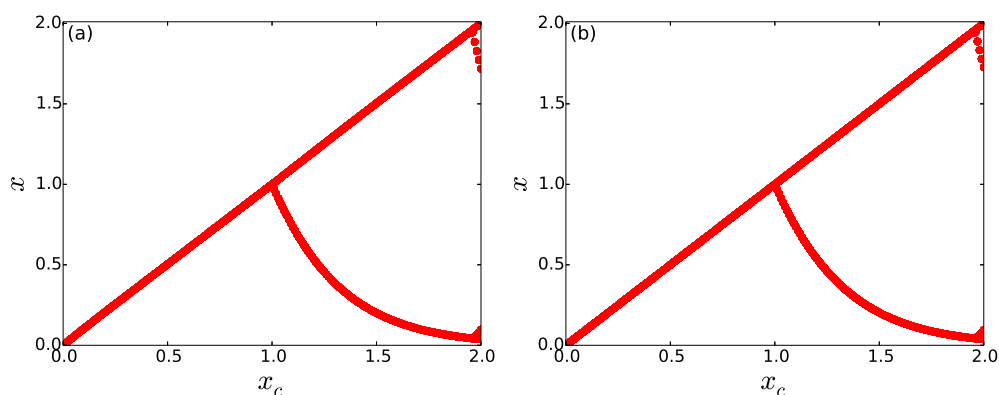


**Fig 2. Bifurcation diagrams of the state of a representative node, with respect to critical threshold  $x_c$ , in a threshold-coupled Random Scale-Free network of intrinsically chaotic populations.** Here  $T_R = 5000$  and the network has a single open node, of degree (a) 1 and (b) 15.

### Influence of the redistribution time and the number of open nodes on the suppression of chaos

Now we focus on the network dynamics when  $T_R$  is small, and the time-scales of the nodal population dynamics and the inter-patch transport are comparable. So now

there will be nodes that may remain over-critical at the time of the subsequent chaotic update, as the system does not have sufficient time to “relax” between population updates. The network is then akin to a rapidly driven system, with the de-stabilizing effect of the chaotic population dynamics competing with the stabilizing influence of the threshold-activated coupling. So for small  $T_R$ , the system does not get enough time to relax to under-critical states and so perfect control to steady states may not be achieved.

Importantly now, the fraction of open nodes  $f^{open}$  is crucial to chaos suppression. In general, a larger fraction of open nodes facilitates control of the intrinsic chaos of the nodal population dynamics, as the de-stabilizing “excess” is transported out of the system more efficiently. We investigate this dependence, through space-time plots of representative networks with varying number of open nodes and redistribution times (cf. Fig. 3), and through bifurcation diagrams of this system with respect to critical threshold  $x_c$  (cf. Fig. 4).

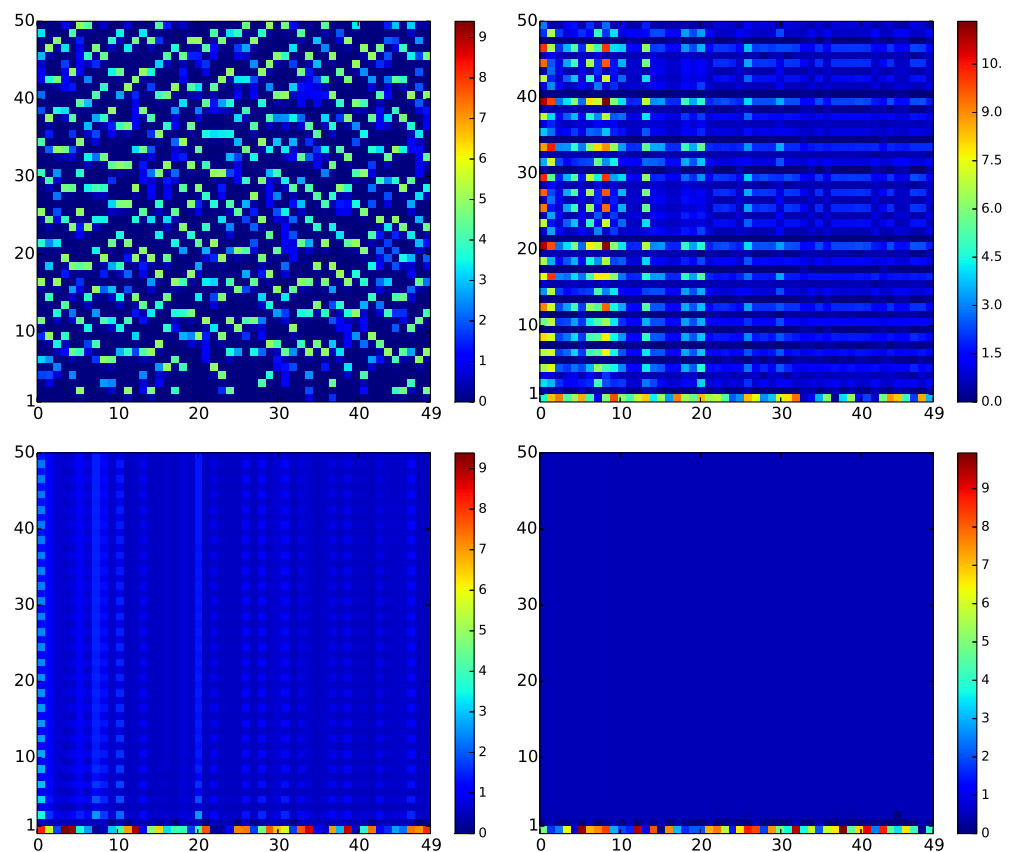


**Fig 3. Space-time plots displaying the spatiotemporal behaviour of a Random Scale-Free network of intrinsically chaotic populations.** Here time runs along the vertical axis and site index displayed along the horizontal axis. Panel (a) shows the case of uncoupled chaotic populations evolving from a representative random initial state. Panels (b), (c) and (d) show the evolution of the same populations connected through threshold-activated coupling. System size  $N = 50$ , redistribution time  $T_R = 50$ , the critical threshold  $x_c = 0.5$  and the number of open nodes in the network is (b) 1, (c) 10, (d) 30.

It is apparent from Fig. 3, that when there are enough open nodes, the network

relaxes to the steady state even for low redistribution times. Also notice from Fig. 3(d) that the system *reaches the steady state very rapidly*, namely within a few time steps, from the random initial state. So more open nodes yields better control of the intrinsic chaos of the nodal population dynamics to fixed populations. This is also corroborated in the bifurcation diagrams displayed in Fig. 4, where control to steady states is seen even for low  $T_R$ , when there are large number of open nodes, vis-a-vis networks with few open nodes. Further contrast this with the dynamics of a system with large  $T_R$ , shown earlier in Fig. 2, where even a *single* open node leads to stable steady states for a large range of threshold values. Similar qualitative trends are also borne out in Random Scale-Free network with  $m = 2$ , where again more open nodes and longer redistribution times result in better control to fixed population densities.

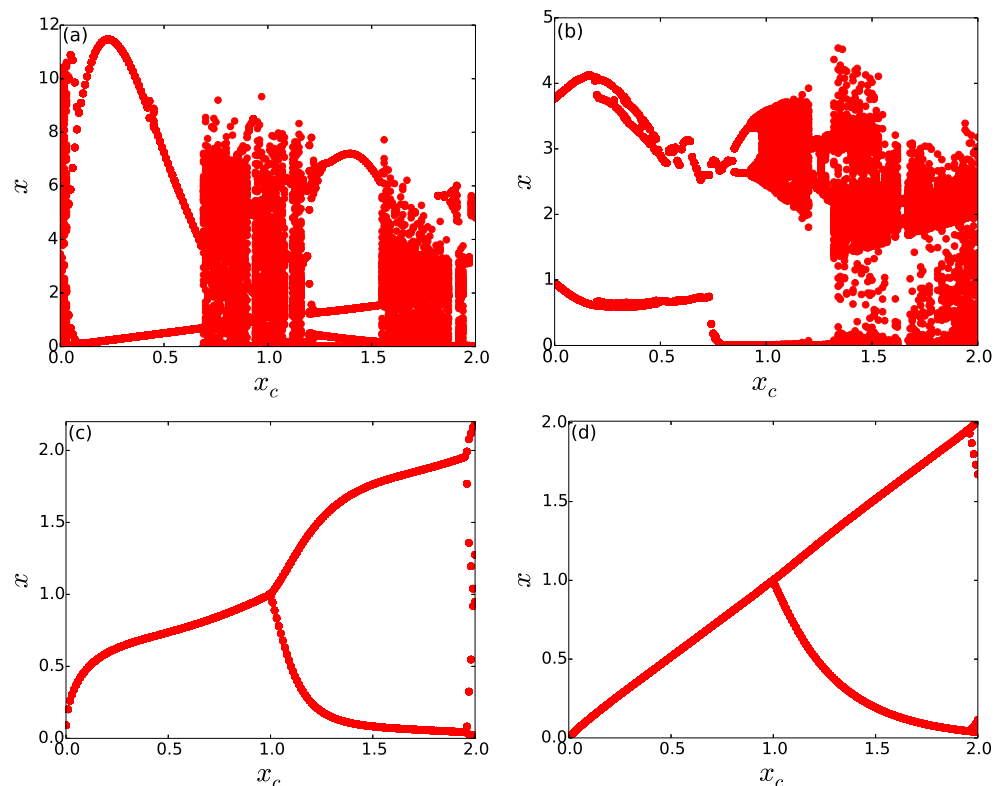


**Fig 4. Bifurcation diagrams for one representative node in a threshold-coupled Random Scale-Free network of intrinsically chaotic populations, with respect to critical threshold  $x_c$ .** Here  $T_R = 50$  and the number of open nodes is (a) 1, (b) 10, (c) 30 and (d) 60.

As a limiting case, we also studied the spatiotemporal behaviour of threshold-coupled networks without open nodes. Here the network of coupled population patches is a closed system. Again the intrinsic chaos of the populations is suppressed to regular behaviour, for large ranges of threshold values. However, rather than steady states, one now obtains period-2 cycles. This is evident through the bifurcation diagram of a closed network (cf. Fig. 5) vis-a-vis networks with at least one open node (cf. Fig. 2). Also, note the similarity of the bifurcation diagram of the closed system with that of a system with low  $T_R$  and few open nodes. This similarity stems from the underlying fact that in both cases the network cannot relax to completely under-critical states by redistribution of excess between the population

updates, either due to paucity of time for redistribution (namely low  $T_R$ ) or due to the absence of open nodes to transport excess out of the system.

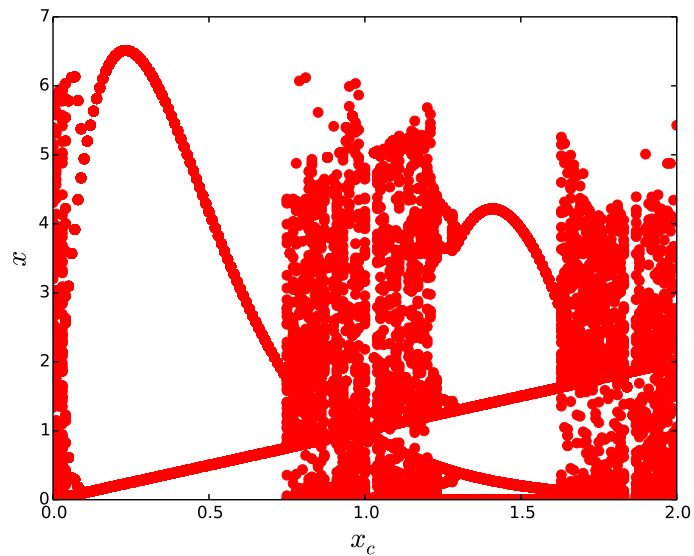


**Fig 5. Bifurcation diagram displaying the state of a representative site, for threshold-coupled populations in a Random Scale-Free network.** Here  $T_R = 5000$  and there are no open nodes.

Lastly, we explore the case of networks with very few (typically 1 or 2) open nodes, and study the effect of the degree and betweenness centrality [23] of these open nodes on the control to steady states. We observe that when there are very few open nodes, the degree and betweenness centrality of the open node is important, with the region of control being large when the open node has the high degree/betweenness centrality, and vice versa. This interesting behaviour is clearly seen in the bifurcation diagrams shown in Figs. 6a-d, which demonstrate that the degree and betweenness centrality of the open node has a pronounced influence on control.

### Quantitative Measures of the Efficiency of Chaos Suppression

We now investigate a couple of quantitative measures that provide indicators of the efficiency and robustness of the suppression of chaos in the network. The first quantity is the average redistribution time  $\langle T \rangle$ , defined as the time taken for all nodes in a system to be under-critical (i.e.  $x_i < x_c$  for all  $i$ ), averaged over a large sample of random initial states and network configurations. So  $\langle T \rangle$  provides a measure of the efficiency of stabilizing the system, and reflects the rate at which the de-stabilizing “excess” is transported out of the network. Fig. 7 shows the dependence of  $\langle T \rangle$  on system size  $N$ . Clearly, while larger networks need longer redistribution times in order to reach steady states, this increase is only logarithmic. This is further corroborated by calculating the average fraction of nodes in the network that go to steady states with respect to the redistribution time  $T_R$ , for networks of different sizes, with varying number of open nodes (cf. Fig. 8). Clearly for small systems, with sufficiently high  $f^{open}$ , very low  $T_R$  can lead to stabilization of all nodes. Importantly, when the fraction of open nodes is very small, the average redistribution time  $\langle T \rangle$  depends sensitively on the betweenness centrality of the open node, and to a lesser extent its degree. Figs. 9a-b present illustrative results demonstrating this observation.

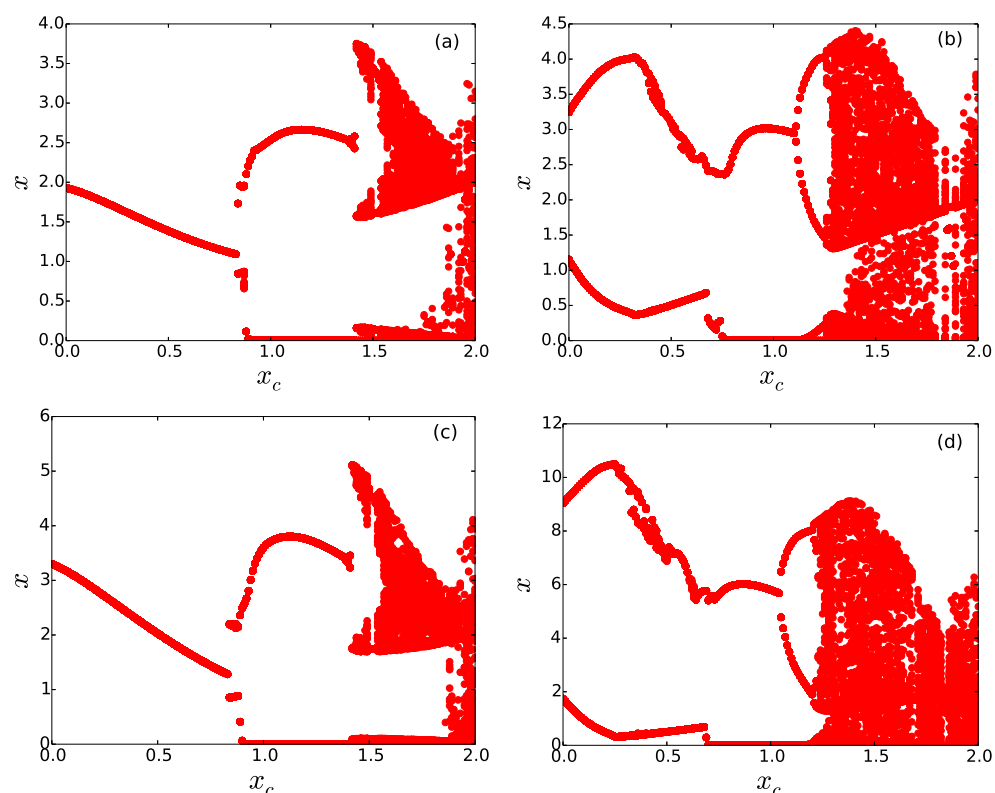


**Fig 6. Bifurcation diagrams displaying the state of a representative node, with respect to critical threshold  $x_c$ , in a threshold-coupled Random Scale-Free network of intrinsically chaotic populations.** Here  $T_R = 500$  and there is a single open node, with this open node having (a) the highest betweenness centrality, (b) the lowest betweenness centrality, (c) the highest degree and (d) the lowest degree in the network.

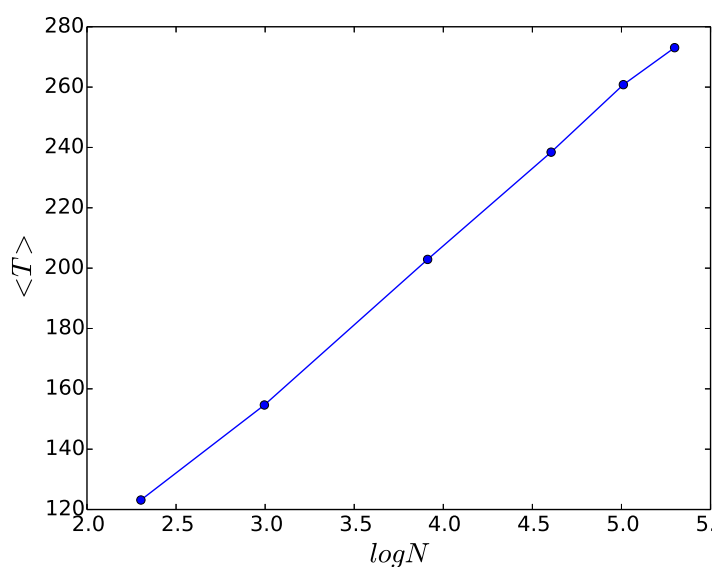


**Fig 7. Average redistribution time  $\langle T \rangle$ , as a function of the logarithm of the network size  $N$ .** Here  $\langle T \rangle$  is defined as the time taken for all nodes in a system to be under-critical (i.e.  $x_i < x_c, \forall i$ ), averaged over a large sample of random initial states and network configurations, the fraction of open nodes in the network is 0.2 and  $x_c = 0.5$ .



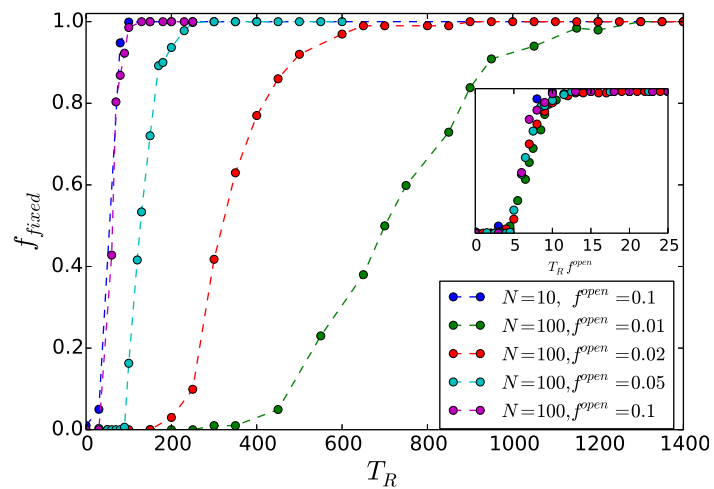


**Fig 8.** Fraction of nodes in the network that go to steady states, denoted by  $f_{fixed}$ , with respect to the redistribution time  $T_R$ . Here  $f_{fixed}$  is averaged over different network configurations and initial states,  $x_c = 0.5$  and the fraction of open nodes  $f^{open}$  in the network is 0.01, 0.02, 0.05, 0.1 for  $N = 100$  (i.e. 1, 2, 5, 10 open nodes in the network respectively) and 0.1 for  $N = 10$  (i.e. 1 open node in the network). *Inset:* data collapse indicating the scaling relation  $f_{fixed} \sim g(T_R f^{open})$ .

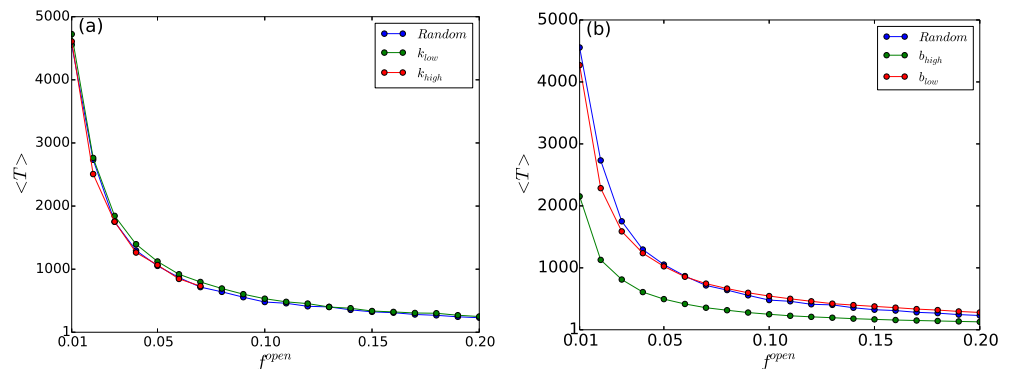


**Fig 9.** Average redistribution time  $\langle T \rangle$ , as a function of the fraction of open nodes in the network  $f^{open}$ . Here  $\langle T \rangle$  is defined as the time taken for all nodes in the threshold-coupled Random Scale-Free Network of chaotic populations, to be under-critical (i.e.  $x_i < x_c, \forall i$ ), averaged over a large sample of random initial states and network configurations. There are 100 chaotic populations connected via threshold-activated transport in a Random Scale-Free network. In panel (a) the case of open nodes chosen in descending order of degree starting from nodes with the highest  $k$  (marked as  $k_{high}$ ) and the case of open nodes chosen in ascending order of degree starting from nodes with the lowest  $k$  (marked as  $k_{low}$ ), are displayed. In panel (b) the case of open nodes chosen in descending order of betweenness centrality starting from nodes with the highest  $b$  (marked as  $b_{high}$ ) and the case of open nodes chosen in ascending order of betweenness centrality starting from nodes with the lowest  $b$  (marked as  $b_{low}$ ), are displayed. In both panels, the case of open nodes chosen at random is also shown for reference.

Next we calculate the *range of threshold values yielding steady states*, averaged over

a large sample of network configurations and initial states, denoted by  $\langle R \rangle$ . Larger  $\langle R \rangle$  implies that steady states will be obtained in a larger window in  $x_c$  space, thereby signalling a more robust control. We have explored the dependence of this quantity on redistribution time  $T_R$ , and also on the fraction of open nodes in the network, denoted by  $f^{open}$ . From Fig. 10 we see that the steady-state window in  $x_c$  rapidly converges to  $\sim 1$  (namely, the range  $0 \leq x_c < 1$ ), as the number of open nodes increases. So the window yielding suppression of chaos is almost independent of the number of open nodes, after a critical fraction of open nodes  $f_c^{open}$ . We observe that  $f_c^{open}$  tends to zero as the redistribution times increases and system size decreases, implying that *very few open nodes are necessary in order to lead the network to a steady state*.

Lastly we explore the scenario of very few open nodes ( $f^{open} \ll f_c^{open}$ ) in greater depth, through the quantitative measures  $\langle R \rangle$  and  $\langle T \rangle$ . In particular, we investigate the limiting case of a *single* open node. Our attempt will be to understand the influence of the degree  $k$  and betweenness centrality  $b$  of the open node on the capacity to suppress chaos. We have already observed the significant effect of the betweenness centrality of the open node on the efficiency of control to steady states through bifurcation diagrams in Fig. 6. This is now further corroborated quantitatively by the dependence of  $\langle R \rangle$  and  $\langle T \rangle$ , displayed in Figs. 11 and 12(b). The effect of the degree of the open node is less pronounced, though it also does have a discernable effect on the suppression of chaos. As evident from Fig. 12(a), when the open node has a higher degree, it has a higher  $\langle R \rangle$ , indicating that open nodes with higher degree yield larger steady state windows.

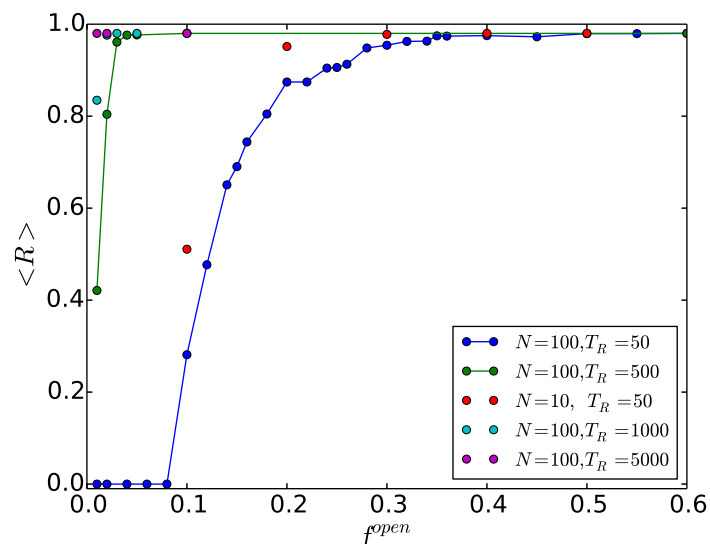


**Fig 10. Range of threshold values that yield steady states,  $\langle R \rangle$ , as a function of the fraction of open nodes in the network  $f^{open}$ .** Here  $\langle R \rangle$  is averaged over different network configurations and initial states and the open nodes are randomly chosen. Results from different redistribution times ( $T_R = 50, 500, 1000, 5000$ ) and system sizes ( $N = 10, 100$ ) are shown.

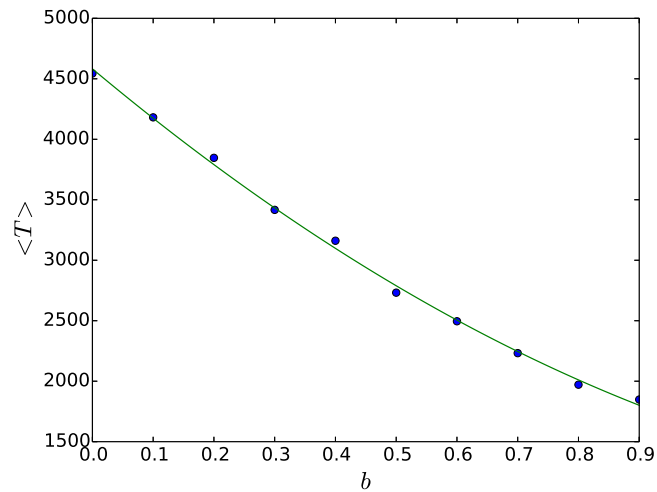


**Fig 11. Average redistribution time  $\langle T \rangle$ , as a function of the betweenness centrality  $b$  of the open node.** Here  $\langle T \rangle$  is defined as the time taken for all nodes in the threshold-coupled Random Scale-Free Network of chaotic populations, to be under-critical (i.e.  $x_i < x_c, \forall i$ ), averaged over a large sample of random initial states and network configurations, in a network with a single open node. The solid curve shows the best quadratic polynomial fit.

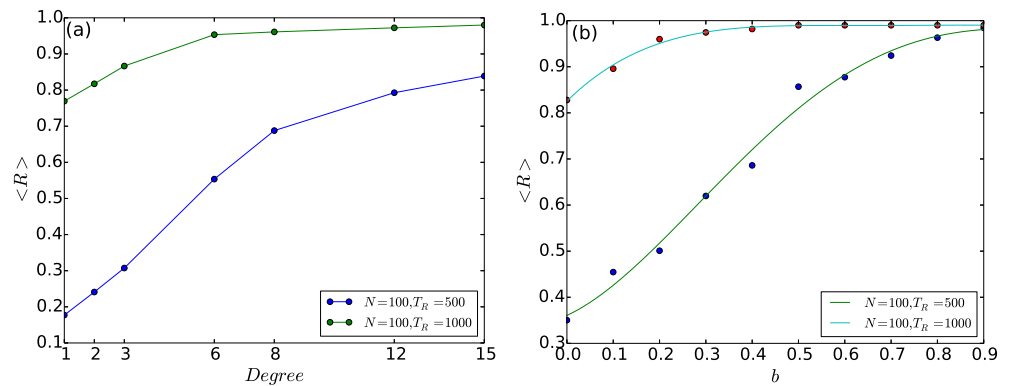


**Fig 12. Range of threshold values that yield steady states  $\langle R \rangle$ , as a function of the (a) degree  $k$ , and (b) betweenness centrality  $b$ , of the open node.** Here  $\langle R \rangle$  is averaged over different network configurations and initial states, in a network with a single open node, (with the solid curve showing the best 4th order polynomial fit).

## Conclusions

We have explored Random Scale-Free networks of populations under threshold-activated transport. Namely we have a system comprising of many spatially distributed sub-populations connected by migrations triggered by excess population density in a patch. We have simulated this threshold-coupled Random Scale-Free network of populations, under varying threshold levels  $x_c$ . We considered networks with varying number of open nodes, namely systems that have different nodes/sites

open to the environment from where the excess population can migrate out of the system. Further, we have studied a range of redistribution times  $T_R$ , capturing different timescales of migration vis-a-vis population change.

Our first important observation is as follows: when redistribution time  $T_R$  is large and the critical threshold  $x_c$  is small ( $0 \leq x_c < 1$ ), we have very efficient control of networks of chaotic populations to steady states. This suppression of chaos and quick evolution to a stable steady states occurs irrespective of the number of open nodes. Further, for threshold values beyond the window of control to fixed states, one obtains cycles of period 2. Namely for threshold levels  $1 < x_c < 2$  the populations evolve in regular cycles, where low population densities alternate with a high population densities. This behaviour is reminiscent of field experiments [22] that show the existence of alternating states. We offer an underlying reason for this behaviour through the analysis of a single threshold-limited map.

For small redistribution time  $T_R$ , the system does not get enough time to relax to under-critical states and so perfect control to steady states may not be achieved. Importantly, now the number of open nodes is crucial to chaos suppression. We clearly demonstrate that when there are enough open nodes, the network relaxes to the steady state even for low redistribution times. So more open nodes yields better control of the intrinsic chaos of the nodal population dynamics to fixed populations. We corroborate all qualitative observations by quantitative measures such as average redistribution time, defined as the time taken for all nodes in a system to be under-critical, and the range of threshold values yielding steady states.

We also explored the case of networks with very few (typically 1 or 2) open nodes in detail, in order to gauge the effect of the degree and betweenness centrality of these open nodes on the control to steady states. We observed that the degree of the open node does not have significant influence on chaos suppression. However, betweenness centrality of the open node is important, with the region of control being large when the open node has the high betweenness centrality, and vice versa.

In summary, threshold-activated transport yields a very potent coupling form in a network of populations, leading to robust suppression of the intrinsic chaos of the nodal populations on to regular steady states or periodic cycles. So this suggests a mechanism by which chaotic populations can be stabilized rapidly through migrations or dispersals triggered by excess population density in a patch.

## Appendix : Analysis of a single population patch under threshold-activated transport

We will now analyze the dynamics of a single Ricker map, modelling a single population patch, under threshold-activated transport. Specifically then we have the following scenario: in the dynamical evolution of the system, if the updated state exceeds a critical threshold  $x_c$ , it transports the excess out of the system and “re-sets” to level  $x_c$ . So the effective map of the dynamics is:

$$x_{n+1} = f(x_n) \quad \text{if } f(x_n) < x_c \quad (2)$$

$$x_{n+1} = x_c \quad \text{if } f(x_n) \geq x_c \quad (3)$$

This is effectively a “beheaded” or “flat-top” map, with the curve lying above  $x_{n+1} > x_c$  in the usual Ricker map being “sliced” to  $x_c$  (cf. Fig. 13a). The level at which the map is chopped off depends on the threshold  $x_c$ . The fixed point solution  $x^*$  occurs at the intersection of this  $f(x)$  curve and the  $45^\circ$  line, namely  $x^* = x_c$ .

Remarkably, this fixed point is *super-stable* if the intersection occurs at the “flat top”, since  $f'(x^*) = 0$  there.

Clearly, as the threshold increases the intersection of the effective map and the  $45^0$  line is no longer located at the “flat-top”. This is clear for the effective maps for  $x_c = 0.5$  vis-a-vis that for  $x_c = 1.5$  in Fig. 13a. So  $x^*$  for sufficiently high  $x_c$  will no longer be stable (eg.  $x_c = 1.5$  will not yield a stable fixed point). So we go on to inspect the second iterate of the effective map, in order to ascertain if a stable period-2 cycle is obtained (cf. Fig. 13b). Now the period-2 cycle solutions occur at the intersection of the  $f^2(x)$  curve and the  $45^0$  line, and again this cycle is stable if and only if the intersection occurs at the “flat top”, namely where  $f'(x) = 0$ . In the illustrative example displayed in Fig. 13b it is clear that for  $x_c = 0.5$ , where the fixed point is super-stable, the period-2 is also naturally super-stable. Interestingly now, for  $x_c = 1.5$ , which had an unstable fixed point solution, the period-2 solution is super-stable. So higher  $x_c$  also controls the intrinsic chaos. However, instead of a stable steady state, it yields stable periodic behaviour.

Alternately, one can understand the emergence of stable cycles under threshold control as follows: The ergodicity of the system ensures that the system will explore the available phase space fully, and the state variable is thus guaranteed to exceed threshold at some point in time. So one can analyse the dynamics of the effective map starting with the initial state at  $x_c$ . Now starting from  $x_c$  the dynamics will run as in the usual Ricker population map until  $x_{n+1} > x_c$ , at which point it is re-set back to  $x_c$  and the cycle starts again. So once it exceeds the critical value it is trapped immediately in a stable cycle whose periodicity is determined by the value of the threshold. Further, this allows us to exactly obtain the values of threshold  $x_c$  that yield stable fixed points  $x^*$  (namely period-1). This is simply the range of  $x_c$  for which the first iterate of the Ricker map lies above  $x_c$ . In this range  $f(x_c) > x_c$ . So starting from an initial state  $x_c$ , we will be updated in the next iterate to a state greater than  $x_c$ , leading to the transport of the excess  $f(x) - x_c$  out of the system and the “relaxation” of the system to  $x_c$ .

The curves  $f_n(x_c)$  as a function of threshold  $x_c$  are displayed in Fig. 14. For  $n = 0$ ,  $f_0(x_c) = x_c$ ; for  $n = 1$ ,  $f_1(x_c) = x_c \exp(r(1 - x_c))$ , and in general  $f_n(x_c) = f \circ f_{n-1}(x_c) = f \circ f \circ \dots \circ f(x_c)$ . From the figure it can be clearly seen that in the range of  $x_c \in [0 : 1]$ ,  $f(x_c) > x_c$ . So if the threshold is in this range, the system will evolve quickly to a steady state at  $x^* = x_c$ , and transport the excess, namely  $f(x_c) - x_c$ , out of the system after every update of the population in the patch.

Similarly, it can be seen that  $f_2(x_c) = f(f(x_c))$  is larger than  $x_c$  (while  $f(x_c) < x_c$ ) in the range of threshold  $x_c \in (1, 2]$ . So in this range of threshold, we obtain a stable period 2 cycle. Namely, the population at  $x_c$  evolves to  $f(x_c) < x_c$  which then evolves to  $f^2(x_c)$ . Since  $f^2(x_c) > x_c$ , it is mapped back to  $x_c$ . Hence a cycle of period 2 arises, with the values of the two points in the cycle being  $x_c$  and  $f(x_c)$ . It can be seen from Fig. 14 that this range is from  $x_c \sim 1$  to  $x_c \sim 2$ . This also corroborates the analysis using effective “flat-top” maps (cf. Fig. 13).

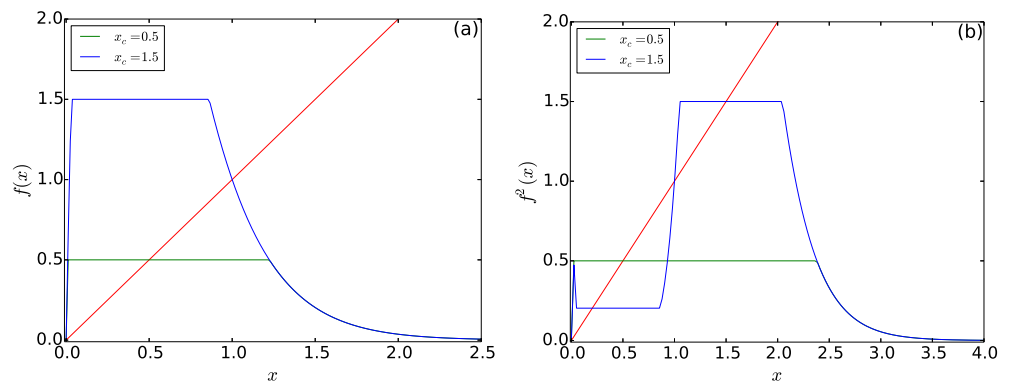


**Fig 13. (a)  $f(x)$  vs.  $x$  and (b)  $f^2(x)$  vs.  $x$ , for the effective threshold-controlled Ricker map ( $r = 4$ ), for critical threshold levels:  $x_c = 0.5$  (green) and  $x_c = 1.5$  (blue).** The fixed point solution occurs at the intersection of the  $f(x)$  curve and the  $45^\circ$  line, and is stable if the intersection occurs at the “flat top”, namely where  $f'(x) = 0$ .

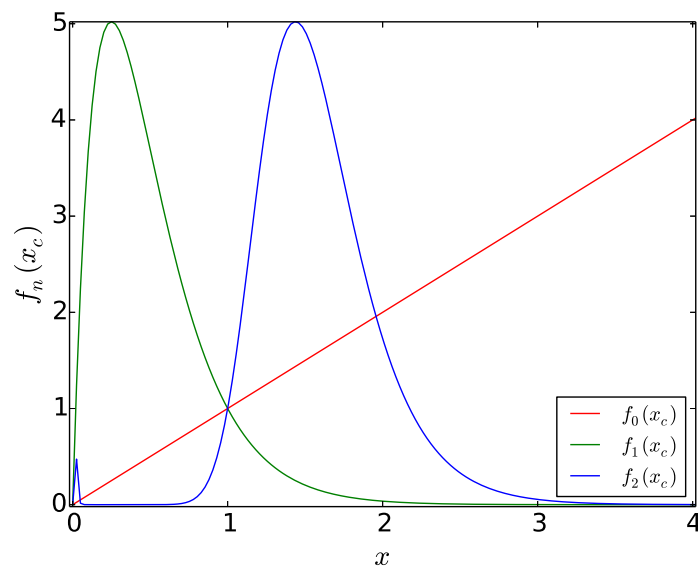


**Fig 14. Plot of  $f_n(x_c)$  vs  $x_c$ .** Here  $n = 0, 1, 2$ , where  $f_n(x_c)$  is the  $n^{th}$  iterate starting from initial condition  $x = x_c$  of the Ricker map with  $r = 4$ :  $f_0(x_c)$  (red),  $f_1(x_c)$  (green) and  $f_2(x_c)$  (blue).

When there is enough time to relax between chaotic updates (namely  $T_R$  is large and/or the number of open nodes is sufficiently high), the collective excess of the network is transported out of the system. This implies that the individual nodes behave essentially like the “flat-top” map analysed here. This explains why the range of threshold values yielding fixed points and period-2 cycles obtained in networks of threshold-coupled chaotic systems (cf. Fig. 2) matches so well with that obtained here (cf. Fig. 15).

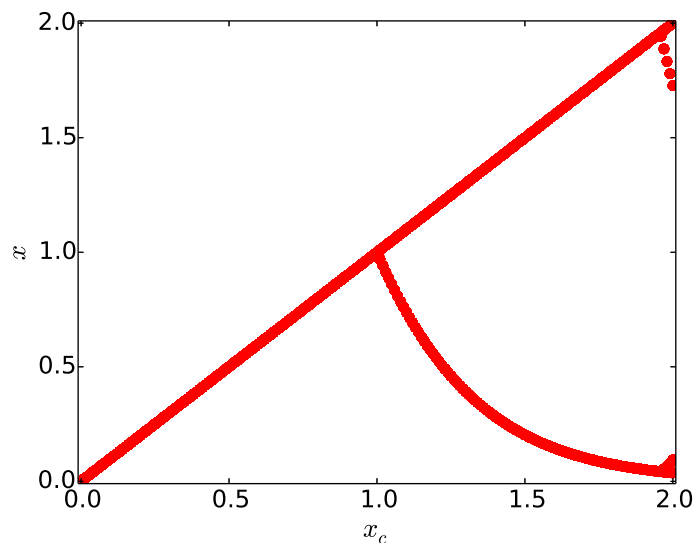


**Fig 15.** Bifurcation diagram of the threshold-controlled Ricker map (namely, the “flat-top” map), with respect to threshold level  $x_c$ .

## References

1. A few representative examples: A. Garfinkel, M. Spano, W. Ditto, J. Weiss, *Science* **257** (1992) 1230; K. Hall et al, *Phys. Rev. Letts.* **78** 4518 (1997).
2. B. A. Huberman and E. Lumer, *IEEE Trans. Circuits Syst.* **37** (1990) 547; S. Sinha, R. Ramaswamy and J. Subba Rao, *Physica D* **43** (1990) 118.
3. E. Ott, C. Grebogi, and J.A. Yorke, *Phys. Rev. Lett.* **64**, 2837 (1990).
4. L. Glass and W. Zheng, *Int. J. Bif. and Chaos*, **4** (1994) 1061.
5. S. Sinha and N. Gupte, *Phys. Rev. E*, **58** (1998) R5221.
6. S.P. Cornelius, W.L. Kath, and A.E. Motter, *Nature communications* **4** (2013).
7. I Hanski, *Nature*, **396**, 41 (1998).
8. C.M. Taylor and R.J. Hall, *Biology Letters*, **8**, 477 (2012).
9. R Levins, *Bulletin of the ESA*, **15**, 237 (1969).
10. V. Colizza, R. Pastor-Satorras and A Vespignani, *Nature Physics* **3**, 276-282 (2007).
11. B Kerr, C Neuhauser, B J M Bohannon & A M Dean, *Nature*, **442**, 75 (2006).
12. JH Brown & A Kodric-Brown, *Ecology*, **58**, 445 (1977).
13. T Reichenbach, M Mobilia & E Frey, *Nature*, **448**, 1046 (2007).
14. B Cazelles, S Bottani & L Stone, *Proc. R. Soc. B*, **268**, 2595 (2001).
15. S. Sinha and D. Biswas, *Phys. Rev. Letts.* **71** (1993) 2010.
16. S. Sinha, *Phys. Rev. E*, **49** (1994) 4832; *Phys. Letts. A*, **199** (1995) 365; *Int. Jour. Mod. Phys. B* **9** (1995) 875.

17. T. Morie, D. Atuti, K. Ifuku, Y. Horio, K. Aihara (2011) 20th European Conference on Circuit Theory and Design (ECCTD), 126-129; G. He, M.D. Shrimali, K. Aihara (2007) *International Joint Conference on Neural Networks*, pp. 350-354.
18. Barabasi, A.-L. and R. Albert, *Science* **286**, 509 (1999).
19. P. Bak, C. Tang and K. Wiesenfeld, *Phys. Rev. Letts.* **59** (1987) 381.
20. A. Mondal and S. Sinha, *Phys. Rev. E* **73** (2006).
21. S. Sinha, *Phys. Rev. E*, **63** (2001) 036212; *ibid*, **69** (2004) 066209; K. Murali and S. Sinha, *Phys. Rev. E*, **68** (2003) 016210.
22. M. Scheffer, S. Rinaldi, A. Gagnani, L. R. Mur, & E. H. van Nes, *Ecology*, **78**, 272 (1997).
23. Betweenness centrality of a node is given as  $b(i) = \sum_{s,t \in I} \frac{\sigma(s,t|i)}{\sigma(s,t)}$ , where  $I$  is the set of all nodes,  $\sigma(s,t)$  is the number of shortest paths between nodes  $s$  and  $t$  and  $\sigma(s,t|i)$  is the number of shortest paths passing through the node  $i$ .